

See discussions, stats, and author profiles for this publication at: <https://www.researchgate.net/publication/51907855>

# Channel-Opening Kinetic Mechanism of Wild-Type GluK1 Kainate Receptors and a C-Terminal Mutant

ARTICLE *in* BIOCHEMISTRY · DECEMBER 2011

Impact Factor: 3.02 · DOI: 10.1021/bi201446z · Source: PubMed

---

CITATIONS

3

---

READS

30

4 AUTHORS, INCLUDING:



**Yan Han**

University of California, Berkeley

13 PUBLICATIONS 216 CITATIONS

SEE PROFILE



**Congzhou Wang**

University at Albany, The State University of ...

17 PUBLICATIONS 139 CITATIONS

SEE PROFILE

Published in final edited form as:

*Biochemistry*. 2012 January 24; 51(3): 761–768. doi:10.1021/bi201446z.

## Channel-Opening Kinetic Mechanism of Wild-Type GluK1 Kainate Receptors and a C-Terminal Mutant

Yan Han<sup>†</sup>, Congzhou Wang, Jae Seon Park, and Li Niu<sup>\*</sup>

Department of Chemistry and Center for Neuroscience Research, University at Albany, SUNY, Albany, New York 12222, United States

### Abstract

GluK1 is a kainate receptor subunit in the ionotropic glutamate receptor family and can form functional channels when expressed, for instance, in HEK-293 cells. However, the channel-opening mechanism of GluK1 is poorly understood. One major challenge to studying the GluK1 channel is its apparent low surface expression, which results in a low whole-cell current response even to a saturating concentration of agonist. The low surface expression is thought to be contributed by an endoplasmic reticulum (ER) retention signal sequence. When this sequence motif is present as in the wild-type GluK1-2b C-terminus, the receptor is significantly retained in the ER. Conversely, when this sequence is lacking, as in wild-type GluK1-2a (i.e., a different alternatively spliced isoform at the C-terminus) and in a GluK1-2b mutant (i.e., R896A, R897A, R900A and K901A) that disrupts the ER retention signal, there is higher surface expression and greater whole-cell current response. Here we characterize the channel-opening kinetic mechanism for these three GluK1 receptors expressed in HEK-293 cells by using a laser-pulse photolysis technique. Our results show that the wild-type GluK1-2a, wild-type GluK1-2b and the mutant GluK1-2b have identical channel-opening and channel-closing rate constants. These results indicate that the C-terminal ER retention signal sequence, which affects receptor trafficking/ expression, does not affect channel-gating properties. Furthermore, as compared with the GluK2 kainate receptor, the GluK1 channel is faster to open, close, and desensitize by at least two-fold, yet the  $EC_{50}$  value of GluK1 is similar to that of GluK2.

Kainate receptor channels are involved in regulating both excitatory and inhibitory neurotransmission.<sup>1–3</sup> Abnormal function of kainate receptors, however, has been implicated in some neurological disorders, such as epilepsy.<sup>4–6</sup> Kainate receptors have 5 subunits, named as GluK1–5.<sup>7</sup> GluK1 (previously known as GluR5),<sup>8</sup> the focus of this study, is alternatively spliced at the C-terminus, producing various receptor isoforms.<sup>8,9</sup> Among them, GluK1-2b is 49 amino acids longer than GluK1-2a, the shortest, whereas GluK1-2c, the longest, is generated by an in-frame insertion of nucleotides encoding for an additional 29 amino acids, into the GluK1-2b sequence (Figure S1).<sup>9</sup>

To date, the understanding of the biophysical properties of kainate receptors at a molecular level emerged largely from studies of GluK2.<sup>2</sup> The kinetic properties of GluK1 receptors are not well understood, in part because of their intrinsic low surface expression. GluK1, like the other kainate receptor subunits GluK2 and 3, can form homomeric channels in a

<sup>\*</sup>Corresponding Author Tel: 518-591-8819. Fax: 518-442-3462. lniu@albany.edu..

<sup>†</sup>Current Address: Department of Molecular and Cellular Physiology, Stanford University School of Medicine, Stanford, CA 94305

**Supporting Information** The supporting information includes a schematic figure showing the C-termini of the GluK1 receptor isoforms, a Hill equation fit to the dose-response relationship, and several tables showing the results of the nonlinear regression data for the best fit of  $n, K_I$  and  $k_{op}$  to the observed rate constant of channel opening as a function of glutamate concentration. This material is available free of charge via the Internet at <http://pubs.acs.org>.

heterologous expression system.<sup>8,9</sup> However, GluK1, when expressed in human embryonic kidney (HEK-293) cells, for instance, produces a low current response to even a saturating concentration of agonist.<sup>9–12</sup> In a study of GluK1, Ren *et al.*<sup>10</sup> identified an endoplasmic reticulum (ER) retention signal from the intracellular C-terminus of GluK1-2b. The motif consists of a series of positively charged residues or mostly arginines. Among them, Arg896 is critical for its ER retention and low surface expression.<sup>10</sup> If this ER retention motif in the wild-type GluK1-2b is disrupted by mutation, the ER exit of the receptor is promoted and the surface delivery is enhanced, resulting in a larger whole-cell current.<sup>10</sup> A sizeable whole-cell current response is essential for studying the biophysical properties of a receptor channel. For instance, properties of the closed-channel conformation are studied at a low agonist concentration, which evokes low current response.<sup>13</sup> A low current response becomes even lower in the presence of an inhibitor. Furthermore, a sizeable whole-cell current response can serve as a functional output at cell surface for studying trafficking of kainate receptors, which is involved in affecting neurotransmission during synaptic plasticity and neuronal development.<sup>1–13</sup>

Here we focus on the wild-type GluK1-2b receptor subunit, wild-type GluK1-2a (which does not contain the ER retention signal, unlike the wild-type GluK1-2b) and a mutant GluK1-2b (R896A, R897A, R900A, K901A). GluK1-2a is a commonly used wild-type isoform representative of GluK1 in various studies.<sup>9, 11, 12, 14, 15</sup> Mutations of mostly arginines within the ER retention signal located in the C-terminus of GluK1-2b are known to abolish ER retention.<sup>10</sup> Therefore, the mutant GluK1-2b receptor lacks the ER-retention signal and is expected to express better than the wild-type GluK1-2b in HEK-293 cells for electrophysiological experiments. The questions we set out to address in this study are: (a) what are the kinetic and equilibrium constants for the opening of the GluK1 channels; (b) does a mutation in the ER-retention signal or the trafficking motif affect these constants; (c) does a GluK1 isoform that lacks the entire ER retention signal (i.e., GluK1-2a) have different channel-opening kinetic constants? To measure these channel-opening constants, we used a laser-pulse photolysis technique with a photolabile precursor of glutamate or caged glutamate,<sup>16</sup> which provides ~60 microsecond ( $\mu$ s) time resolution.<sup>17–19</sup>

## EXPERIMENTAL PROCEDURES

### Expression of cDNAs and Cell Culture

The DNA plasmids encoding the wild-type GluK1-2a(Q), wild-type GluK1-2b(Q) and the mutant GluK1-2b (R896A, R897A, R900A, K901A) were respectively from Peter Seeburg and Geoffrey Swanson. The 3132-bp fragment harboring the open reading frame that encodes GluK1-2a was cloned into pcDNA3.1(+). The cDNA plasmids were propagated through an *E. coli* host (DH5 $\alpha$ ) and purified using a QIAGEN kit. A receptor was transiently expressed in HEK-293 cells by a calcium phosphate method, as previously described.<sup>17</sup> The HEK-293 cells were also cotransfected with a DNA plasmid encoding green fluorescent protein and another plasmid encoding the SV40 large T-antigen.<sup>17</sup> The weight ratio of the DNA plasmid for a receptor to green fluorescent protein to large T-antigen was 20:1:2, with the receptor DNA plasmid being 20  $\mu$ g per 35-mm Petri dish. The cells were cultured in Dulbecco's modified Eagle medium supplemented with 10% fetal bovine serum and 1% penicillin in a 37 °C, 5% CO<sub>2</sub>, humidified incubator. Transfected cells were allowed to grow for at least 48 h before recording.

### Whole-Cell Current Recording

Electrodes for whole-cell recording were made from glass capillaries from World Precision Instruments (Sarasota, FL) and fire polished. The electrode had a resistance of ~3 M $\Omega$  when filled with the pipette solution. The pipette solution contained (in mM) 110 CsF, 30 CsCl, 4

NaCl, 0.5 CaCl<sub>2</sub>, 5 EGTA, and 10 HEPES (pH 7.4 adjusted by NaOH). The external cellular solution contained (in mM) 150 NaCl, 3 KCl, 1 CaCl<sub>2</sub>, 1 MgCl<sub>2</sub>, and 10 HEPES (pH 7.4 adjusted by NaOH). Green fluorescence in the transfected cells was visualized using a Carl Zeiss Axiovert S100 microscope equipped with a fluorescent detection system (Thornwood, NY). The glutamate-induced whole-cell current was recorded using an Axopatch200B amplifier at a cutoff frequency of 2–20 kHz by a built-in, 4-pole low-pass Bessel filter and was digitized at 5–50 kHz sampling frequency using a Digidata 1322A from Molecular Devices (Sunnyvale, CA). Data were acquired by using pClamp 8 software (also from Molecular Devices). All data were collected from the transfected HEK-293 cells voltage-clamped at –60 mV and 22 °C.

### Laser-Pulse Photolysis Measurement

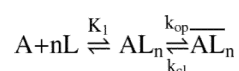
In the laser-pulse photolysis measurement,  $\gamma$ -O-( $\alpha$ -carboxy-2-nitrobenzyl)glutamate or caged glutamate (Invitrogen)<sup>16–18</sup> was photolyzed to liberate glutamate for measuring the rate of GluK1 receptor channel opening. We also used another caged glutamate, i.e., 4-methoxy-7-nitroindolyl-glutamate,<sup>20</sup> for some of our measurements. We tested the two caged glutamate compounds extensively with several glutamate receptor channels and found no difference in the rate constant measurement. Caged glutamate (or free glutamate) was applied to an HEK-293 cell suspended in the extracellular solution by using a U-tube flow device.<sup>17, 18</sup> The cell was equilibrated with caged glutamate for 250 ms before being irradiated by a laser pulse. A Minilite II pulsed Q-switched Nd:YAG laser (Continuum, Santa Clara, CA), tuned by a third harmonic generator, produced single pulses of 8 ns at 355 nm. The laser light was introduced to a cell via a fiber optic, and the power was adjusted to 200–800  $\mu$ J. For a laser-pulse photolysis measurement of a channel-opening kinetic rate constant, we also used at least two known concentrations of free glutamate with the same cell before and after a laser flash to calibrate the concentration of photolytically released glutamate.<sup>17, 18, 21</sup> The current amplitudes obtained from flow measurements were compared with that of the laser measurement with reference to the dose-response relationship. The flow measurement also allowed us to monitor any potential damage to the receptors and/or the cell for successive laser flashes with the same cell.

### Data Analysis

In the laser-pulse photolysis measurement of the channel-opening reaction, we observed that the whole-cell current rise followed a single-exponential rate process (>95%) over the entire range of ligand (glutamate) concentrations that we were able to measure (i.e., 60–400  $\mu$ M glutamate or ~4% – 52% of the fraction of the open-channel population; see the dose-response curve in the Results). Therefore, the observed rate constant of channel opening,  $k_{obs}$ , was empirically determined by eq 1

$$I_t = I_A (1 - e^{-k_{obs}t}) \quad (1)$$

where  $I_t$  and  $I_A$  represent the whole-cell current amplitude at time  $t$  and the maximum current amplitude, respectively. To describe the relationship between  $k_{obs}$  and agonist concentration, we introduced a general mechanism of channel opening.<sup>17, 18, 21</sup>



Here,  $A$  stands for the active, unliganded form of the receptor,  $L$  the ligand or glutamate,  $AL_n$  the closed-channel state with  $n$  ligand molecules bound, and  $\overline{AL_n}$  the open-channel state. The

number of glutamate molecules to bind to the receptor and to open its channel,  $n$ , can be from 1 to 4, assuming that a receptor is a tetrameric complex and each subunit has one glutamate binding site.<sup>22–26</sup> It is further assumed that a ligand does not dissociate from the open-channel state. The  $k_{op}$  and  $k_{cl}$  are the channel-opening and channel-closing rate constants, respectively. For simplicity and without contrary evidence, it is assumed that glutamate binds at all binding steps with equal affinity or  $K_I$ , the intrinsic equilibrium dissociation constant. By this mechanism, eq 2 was derived.

$$k_{obs} = k_{cl} + k_{op} \left( \frac{L}{L + K_I} \right)^n \quad (2)$$

In deriving eq 2, the rate of ligand binding was assumed to be fast relative to the rate of channel opening. This assumption is consistent with kinetic evidence that the whole-cell current rise (described in detail in the Results) follows a first-order rate law (eq 1) not only in this study but also in all of our previous studies of the channel-opening mechanism for other kainate receptors.<sup>18</sup> From eq 2, a set of  $k_{cl}$  and  $k_{op}$  values as well as  $K_I$  were found to be correlated with a particular number of ligands ( $n$ ) that bound to and subsequently opened the receptor channel.

Furthermore,  $K_I$  was independently estimated from the dose-response relationship, as in eq 3, which was also derived based on the general mechanism of channel opening described above. In eq 3,  $I_M$  is the current per mole of receptor,  $R_M$  is the number of moles of receptors on the cell surface, and  $\Phi^{-1}$  is the channel opening equilibrium constant.

$$I_A = I_M R_M \frac{L^n}{L^n + \Phi(L + K_I)^n} \quad (3)$$

It should be noted that  $n$  as in both eqs 2 and 3 is the number of glutamate molecules to bind to and open the channel, and is not the Hill coefficient. Like the Hill equation,<sup>27</sup> eq 3 accounts for macroscopic current response to the entire range of agonist concentration. As such, eq 3, together with eq 2, does not take into account the contribution of different conductance levels and the change of conductance with increasing agonist occupation. Nonetheless, we found that the best fitted value of  $n$  to be 2 from the use of eq 2 and eq 3, as described in Results.

Unless otherwise noted, each data point shown in the plots of this study was an average of at least three measurements collected from at least three cells. Linear regression and nonlinear fitting were performed using Origin 7 (Origin Lab, Northampton, MA). Unless otherwise noted, standard error of the mean was reported.

## RESULTS

### Expression and Detection of Wild-Type GluK1-2a, Wild-type GluK1-2b and the Mutant GluK1-2b Channels by Whole-Cell Recording

We expected that the mutant GluK1-2b has a higher expression level and thus higher current amplitude than the wild-type GluK1-2b for the following reason: The mutant GluK1-2b was constructed to change the amino acid sequence of its ER retention signal so that its ER exit and surface expression would be enhanced compared with the wild-type GluK1-2b<sup>10</sup>. On the other hand, GluK1-2a does not contain the alternatively spliced C-terminal domain or the ER retention signal that exists in the wild-type GluK1-2b sequence. If the ER retention sequence motif regulates only the receptor trafficking and cell surface expression, we expect

that the wild-type GluK1-2a, wild-type GluK1-2b and the mutant GluK1-2b all have similar, if not identical, gating properties.

To test this hypothesis, we first measured the whole-cell current response of each of the receptors individually expressed in HEK-293 cells. As shown (Figure 1A), whole-cell current responses to glutamate at various concentrations initially increased as a result of channel activation, and then decreased towards baseline due to channel desensitization. Using the amplitude of whole-cell current (Figure 1B), we compared the relative surface expression level for the three receptors in HEK-293 cells. For this comparison, a total of 28 cells expressing the wild-type GluK1-2a, 11 cells expressing the wild-type GluK1-2b, and 15 cells expressing the mutant GluK1-2b were used, and the amount of plasmid we used for transient transfection was the same (24  $\mu$ g per 35-mm dish).

The average whole-cell current amplitude at each of the three glutamate concentrations (0.05, 0.2 and 3 mM) for the mutant GluK1-2b was >5-fold larger than the wild-type GluK1-2b (Figure 1B). The highest current response, as we observed, of the GluK1-2b mutant to 3 mM glutamate is ~2 nA. These observations are comparable with those reported by Ren *et al.*<sup>10</sup> previously. In the study by Ren *et al.*,<sup>10</sup> the GluK1-2b mutants tested contain at most three mutations (i.e., R896A, R900A, K901A). The mutant we tested contains an additional mutation or R896A besides R897A, R900A and K901A. Furthermore, the average of the whole cell current amplitude for the wild-type GluK1-2a was only slightly higher than the wild-type GluK1-2b (Figure 1B). The average whole-cell current response of GluK1-2a to 3 mM glutamate in our experiments (Figure 1B) was only ~800 pA. This value is comparable with those documented in the literature, i.e., 300–800 pA.<sup>6, 9, 12, 14, 28</sup> This result may suggest a different regulatory process for surface expression of GluK1-2a<sup>10</sup>.

### Dependence of the Whole-Cell Current Response on Glutamate Concentration

The dose-response relationship for the two wild-type and the mutant GluK1 receptors was characterized in order to estimate the  $K_I$  (i.e., the intrinsic equilibrium dissociation constant of the ligand) and the  $EC_{50}$  value. As seen in Figure 2A, the dose-response relationships of the wild-type GluK1-2a, wild-type GluK1-2b and the mutant 1–2b receptors were statistically indistinguishable. Quantitatively, the best fit of the combined dose-response data by eq 3 yielded  $K_I$  of  $480 \pm 50$   $\mu$ M (Figure 2A and Table 1) with  $n = 2$  (here  $n$  represents the number of ligand molecules bound to the receptor to open the channel; Table 1 also contains the best fit values of  $K_I$  for  $n = 1, 3$ , and 4). When the dose-response curve was analyzed separately using the same approach,  $K_I$  was  $400 \pm 170$   $\mu$ M for the wild-type GluK1-2a,  $470 \pm 130$   $\mu$ M for the wild-type GluK1-2b, and  $530 \pm 140$   $\mu$ M for the mutant receptor, respectively (data not shown). From the same dose-response data, we also estimated the  $EC_{50}$  value by the Hill equation.<sup>27</sup> We found that  $EC_{50} = 460 \pm 34$   $\mu$ M, and the Hill coefficient =  $1.1 \pm 0.1$  (Figure S2) for the combined dose-response data. When the dose-response relationships of the two wild-type and the mutant GluK1 receptors were analyzed separately, the  $EC_{50}$  value and the Hill coefficient were  $510 \pm 40$   $\mu$ M and  $1.2 \pm 0.1$  for the wild-type GluK1-2a,  $415 \pm 30$   $\mu$ M and  $1.0 \pm 0.1$  for the wild-type GluK1-2b, and  $570 \pm 70$   $\mu$ M and  $1.1 \pm 0.1$  for the mutant GluK1-2b, respectively (data not shown). Based on these results, we concluded that the wild-type and mutant GluK1-2b as well as the wild-type GluK1-2a had an identical dose-response relationship. They also had the same  $n$  value from the best fit, namely, the number of glutamate molecules bound to and open the channel was 2. This value was corroborated by the fitting of both the dose-response data (Figure 2A, Table 1) and the channel-opening rate data, described below. Furthermore, the  $EC_{50}$  value of  $510 \pm 40$   $\mu$ M for GluK1-2a, which we determined, is similar to the  $EC_{50}$  of 631  $\mu$ M for the same receptor reported by Sommer *et al.*<sup>9</sup> (Table S1). However, no  $EC_{50}$  value for GluK1-2b or any of its mutants has been previously reported.



## Dependence of Desensitization Rate Constant on Glutamate Concentration

Next we examined the desensitization rate (as shown in Figure 1A). The desensitization proceeded with a single, first-order rate process for >98% of the reaction and for the entire range of glutamate concentrations for all three receptors. The desensitization rate constant, or  $k_{des}$ , for the two wild-type receptors and the mutant GluK1 increased with increasing glutamate concentration but reached a plateau around 5 mM glutamate (Figure 2B). We found that the channel-desensitization rate profile or the dependence of the channel desensitization rate constant on glutamate concentration appeared to be identical (Figure 2B). The maximum  $k_{des}$  was  $464 \text{ s}^{-1}$  for the wild-type GluK1-2a,  $450 \text{ s}^{-1}$  for the wild-type GluK1-2b and  $457 \text{ s}^{-1}$  for the mutant (Figure 2B), respectively. These results showed that all three receptors desensitized with an identical rate constant at any given glutamate concentration (Figure 2B). Therefore, our results suggest that the difference in the amino acid sequence among the wild-type GluK1-2a, wild-type GluK1-2b and the mutant GluK1-2b (Figure S1) did not affect the channel desensitization kinetics.

The maximum  $k_{des}$  of  $464 \text{ s}^{-1}$  for the wild-type GluK1-2a we determined is in good agreement with the rate constant for the fast-desensitizing process of the same receptor reported previously.<sup>15</sup> We did not, however, observe a slow-desensitizing rate as previously documented<sup>15</sup> (note that the total number of cells we recorded was 28). The magnitude of the  $k_{des}$  that we determined for the mutant GluK1-2b of  $457 \text{ s}^{-1}$  is also similar to the value reported by Ren *et al.*<sup>10</sup> for another GluK1-2b mutant with three point mutations (i.e., R896A, R900A, K901A). We did observe that ~20% of cells (from a total of 20 cells) that expressed the wild-type GluK1-2b showed a slower desensitization rate. The rate constant for the slow desensitization rate was 3.8-fold, 4.0-fold and 4.4-fold smaller collected at 50  $\mu\text{M}$ , 200  $\mu\text{M}$  and 3 mM glutamate concentrations, respectively (data not shown). However, on average, our ratio is ~2-fold larger than the one reported earlier.<sup>15</sup> In contrast, only one cell (out of 25 cells) that expressed the mutant GluK1-2b exhibited a slower rate of desensitization. It should be noted that we did not study any of these slow-desensitizing cells that expressed either the wild-type GluK1-2b or its mutant.

## Channel-Opening Rate Constants

Using the laser-pulse photolysis technique,<sup>17</sup> we measured the channel-opening ( $k_{op}$ ) and channel-closing ( $k_{cl}$ ) rate constants for the wild-type GluK1-2a, wild-type GluK1-2b and the mutant GluK1-2b receptors. The magnitude of  $k_{op}$  reflects how fast a channel opens after the binding of agonist, whereas the magnitude of  $k_{cl}$  reflects how long a channel stays open or the lifetime of the open channel.<sup>19</sup> Therefore, a putative difference between rate constants would be attributed to the difference in the amino acid sequence of the C-termini among the three receptors (Figure S1).

As seen in an example (Figure 3A), laser-pulse photolysis of the caged glutamate triggered a rapid rise of whole-cell current. The time course of the rising phase (Figure 3A), represented by an observed rate constant of channel opening, or  $k_{obs}$ , was adequately described by a single exponential rate process (see the solid line as the fit to this rate process in Figure 3A by eq 1). Various  $k_{obs}$  values were obtained as a function of the concentration of photolytically released glutamate. Inspection of these  $k_{obs}$  values in relation to the range of glutamate concentrations showed that there was not a statistically significant difference among the two wild-type and the mutant GluK1 channels (Figure 3B). The best fit, using eq 2, of  $k_{obs}$  as a function of the glutamate concentration, based on the combined data from the mutant and the two wild-type receptors, yielded that  $n$  was 2, and the  $k_{op}$  and  $k_{cl}$  values were  $(2.6 \pm 0.1) \times 10^4 \text{ s}^{-1}$  and  $(1.1 \pm 0.2) \times 10^3 \text{ s}^{-1}$ , respectively (Figure 3B and Table 2). If the rate data were analyzed separately, the best fit yielded  $k_{op}$  and  $k_{cl}$  of  $(2.2 \pm 0.2) \times 10^4 \text{ s}^{-1}$  and  $(0.9 \pm 0.2) \times 10^3 \text{ s}^{-1}$  for the wild-type GluK1-2a,  $(2.4 \pm 0.1) \times 10^4 \text{ s}^{-1}$  and  $(1.4 \pm 0.2) \times$

$10^3 \text{ s}^{-1}$  for the wild-type GluK1-2b, and  $(0.8 \pm 0.3) \times 10^4 \text{ s}^{-1}$  and  $(2.6 \pm 0.3) \times 10^3 \text{ s}^{-1}$  for the mutant GluK1, respectively, at  $n = 2$ . We therefore conclude that GluK1-2a, GluK1-2b and the GluK1-2b mutant had identical  $k_{op}$  and  $k_{cl}$  values. These results suggest that the difference in the amino acid sequence located in the C-terminal tail that defines the wild-type GluK1-2a and the ER retention signal motif as in the wild-type sequence of GluK1-2b (Figure S1) does not affect the channel-opening rate process (Figure 3B, and Table 2).

### Estimation of (a) the Minimal Number of Glutamate Molecules Bound to a Receptor to Open its Channel and (b) the $K_I$ Value Using the Rate Data

In the study described above (Figure 3), we measured  $k_{obs}$  for the two wild-type receptors and the mutant GluK1 using up to 400  $\mu\text{M}$  of glutamate generated by laser photolysis, which correlated with up to 52% of the fraction of the open-channel population. The wide range of  $k_{obs}$  values vs. glutamate concentration permitted us to simultaneously evaluate, by eq 2,  $k_{op}$  and  $K_I$  as well as  $n$ , the number of glutamate molecules bound to the receptor to open the channel. To achieve a better estimate of  $n$ ,  $K_I$ , and  $k_{op}$  by nonlinear regression using eq 2, we decided to first fix the value of  $k_{cl}$ . This is reasonable because when  $L \ll K_I$ , eq 2 can be reduced to  $k_{obs} \approx k_{cl}$ , suggesting that (a)  $k_{obs}$  at a low glutamate concentration would reflect  $k_{cl}$ , and (b) the value of  $k_{cl}$  is independent of the  $n$  value, as in eq 2.<sup>19, 29</sup> Based on this rationale, we identified  $k_{obs}$  of  $1,000 \text{ s}^{-1}$ , determined at  $\sim 60 \mu\text{M}$  glutamate concentration or  $\sim 4\%$  fraction of the open channel,<sup>19</sup> to be  $k_{cl}$  for the wild-type and mutant GluK1 receptors. By nonlinear regression with  $k_{cl} = 1,000 \text{ s}^{-1}$ , the  $n$  values turned out to be consistently close to 2 (Table S2). Furthermore, choosing  $k_{cl}$  values different from  $1,000 \text{ s}^{-1}$  did not significantly affect the output of  $n$ ,  $K_I$  or  $k_{op}$  values (Table 3). These results are therefore consistent with  $n = 2$  being the best fit (Table 3). This conclusion is also consistent with results from our study of other kainate receptor channels.<sup>17, 19, 21, 30</sup> Furthermore, as is known for kainate receptors, channel activation via a subset of subunits instead of all four in a tetrameric complex can indeed occur.<sup>31</sup> Thus, we favor an interpretation of  $k_{op}$  and  $k_{cl}$  at  $n = 2$  being the representative values of the channel-opening and channel-closing rate constants for the wild-type GluK1-2a, wild-type GluK1-2b and the mutant GluK1-2b receptors.

The evaluation of  $n$  as described above was based on the channel-opening rate data, independent of the analysis of the dose-response relationship (as in Figure 2A). Using the same rate data, we also independently evaluated  $K_I$ , the intrinsic equilibrium dissociation constant (see the scheme in Experimental Procedures). Specifically, nonlinear regression of  $k_{obs}$  vs. glutamate concentration using eq 2 yielded an average of  $K_I$  of  $400 \pm 150 \mu\text{M}$  for the wild-type GluK1-2a, wild-type GluK1-2b and the mutant GluK1-2b receptors (Table S1). This value was in good agreement with the  $K_I$  value of  $480 \pm 50 \mu\text{M}$  obtained from the dose-response measurement (Figure 2A and Table 1). When  $K_I$  was further constrained to be  $480 \mu\text{M}$ , in addition to a fixed  $k_{cl}$ , the fitted values of  $n$  were, again, close to 2, and the fitted values of  $k_{op}$  were relatively invariant, the average of which was  $2.6 \times 10^4 \text{ s}^{-1}$  (Table S3). Finally, if  $k_{cl}$  and  $n$  were kept at  $1,000 \text{ s}^{-1}$  and 2, respectively, we obtained  $k_{op} = 2.1 \times 10^4 \text{ s}^{-1}$  on average. Similarly,  $K_I$  was found to be  $380 \mu\text{M}$  (Table S4). It should be noted that the  $K_I$  value, which was obtained from the channel-opening rate data, was also in agreement with the  $K_I$  value obtained independently from the dose-response relationship.

### Measurement of the Channel-Opening Rate Constant

To characterize the mechanism of channel opening for the GluK1 receptors, we took into account several experimental observations in our kinetic data analysis to obtain  $k_{op}$  and  $k_{cl}$ . For example, the rising phase of the whole-cell current (as in Figure 3A) proceeded with a single exponential rate law in the entire concentration range of glutamate (i.e., 60–400  $\mu\text{M}$ ). This observation was consistent with the assumption that the channel-opening rate or the



rate of transition from the closed-channel form,  $AL_n$ , to the open-channel form,  $\overline{AL_n}$ , was slow compared with all preceding steps involving glutamate binding. On the basis of this assumption, eq 2 was derived. If the channel-opening rate was either comparable to or faster than the ligand-binding rate, a single-exponential rate law would fail. For instance, when the ligand concentration is too low such that the ligand association rate dominates the rate process, the rising phase of the current will represent a bi-molecular association rate process instead.<sup>19, 30</sup> To ensure that ligand binding was fast even at low glutamate concentrations, we did not use any  $k_{obs}$  values at any glutamate concentrations lower than ~4% of the fraction of the open-channel form.<sup>19</sup> For GluK1 receptors, 4% of the fraction of the open-channel form correlates with ~60  $\mu$ M of glutamate (see the dose-response relation). Under this condition  $k_{obs}$  reflected mainly  $k_{cl}$ .<sup>19</sup> To demonstrate that the method of data analysis used here is valid, we note that the  $k_{cl}$  values,<sup>19, 30</sup> calculated using eq 2 and by using ~4% of the fraction of the open-channel form, are generally in agreement with the lifetimes determined by single-channel recording of the same  $\alpha$ -amino-3-hydroxy-5-methyl-4-isoxazolepropionic acid (AMPA) channels with glutamate as the agonist (i.e.,  $k_{cl} = 1/\tau$  and  $\tau$  is the lifetime expressed as time constant).<sup>17, 19, 24, 32</sup>

Swanson *et al*<sup>33</sup> previously studied the homomeric GluK1 receptors using single-channel recording. In the presence of domoate as the agonist, GluK1 channels exhibited three conductance states, and two time constants, i.e., 0.3 ms and 0.7 ms, from the best fit of the open-time distribution. These time constants are equivalent to the rate constants of ~3,300  $s^{-1}$  and 1,400  $s^{-1}$ , respectively. However, no single-channel study of any GluK1 receptors using glutamate as the agonist has been reported thus far. Furthermore, the  $k_{op}$  and  $k_{cl}$  values of GluK1 receptor channels we determined in this study, together with  $K_I$  and  $EC_{50}$  and  $n$  values, were based on macroscopic current response to glutamate. Consequently, the  $k_{op}$  and  $k_{cl}$  values only reflect the average rate constants of an ensemble of single channels or they do not correlate to kinetic constants of individual channels of the ensemble.

## DISCUSSION

In this study, we characterized the channel-opening mechanism for three kainate receptors, namely the wild-type GluK1-2a, wild-type GluK1-2b and a GluK1-2b receptor mutated at the C-terminal tail such that the ER retention signal is disrupted. As expected, the wild-type GluK1-2a and the GluK1-2b mutant receptors that lack the ER retention signal motif are expressed better in HEK-293 cells than the wild-type GluK1-2b. Furthermore, the wild-type GluK1-2a and the mutant GluK1-2b share identical  $k_{des}$ ,  $k_{op}$ ,  $k_{cl}$  and  $K_I$ , as well as  $EC_{50}$  values with the wild-type GluK1-2b. The minimal number of glutamate molecules that bind to any one of the three receptors in order to open the channel is two. Because all three GluK1 receptors have different amino acid sequences in the C-terminal region but identical sequences elsewhere, our results suggest that the C-terminal region, precisely the sequence surrounding the ER-retention and trafficking signal, does not affect the channel-gating properties of GluK1. Our results therefore demonstrate that the GluK1-2b mutant can be used to represent the GluK1-2a and GluK1-2b wild-type receptors in studying their structure-function relationships. Having a better expressed mutant and consequently larger whole-cell current response would be further advantageous for studying the function and the regulation of the GluK1 receptors. The fact that the mutant GluK1-2b receptor produces larger current response but has identical kinetic properties to those of the wild-type GluK1-2a and GluK1-2b further suggests a possibility of finding additional mutants, by changing the amino acid sequences within or near the ER retention/trafficking signal, that express even better in HEK-293 cells and produce an even larger whole-cell current response.

The results from this study using the rat GluK1 receptor now allow us to make comparisons with results obtained for the rat GluK2, the most studied and the best understood kainate receptor channel to date.<sup>12, 18, 21, 34–37</sup> The  $K_I$  of  $300 \pm 210 \mu\text{M}$  for the rat GluK2 defined previously<sup>21</sup> is similar to the  $K_I$  of  $400 \pm 150 \mu\text{M}$  (from the analysis of the combined rate-constant data) and the  $K_I$  of  $480 \pm 50 \mu\text{M}$  for the rat GluK1 (from the analysis of the combined dose-response relation data), suggesting that there is no significant difference between the dose-response relationships of GluK1 and GluK2. Because the peak concentration of glutamate in the synapse cleft is thought to be about 1 mM,<sup>38, 39</sup> both GluK1 and GluK2 kainate receptors can open up to 80% of the receptors under this condition. In other words, both receptors have equal sensitivity to glutamate.<sup>21</sup> Conversely, the channel-opening and channel-closing rate constants of GluK2, i.e.,  $(6.4 \pm 0.3) \times 10^3 \text{ s}^{-1}$  and  $(3.9 \pm 0.3) \times 10^2 \text{ s}^{-1}$ , respectively,<sup>21</sup> are several-fold smaller than those of the GluK1 receptors reported here. This comparison suggests that the GluK1 channels open, in response to glutamate, and close several-fold faster than the GluK2 receptor channel. Furthermore, the maximum desensitization rate constant of the GluK1 channels we report here is almost two-fold larger than that of the rat GluK2 channels<sup>21</sup> (i.e.,  $k_{des} = \sim 460 \text{ s}^{-1}$  vs.  $\sim 230 \text{ s}^{-1}$ ). Taken together, our results show that the GluK1 homomeric receptor is a faster kainate channel followed by the binding of glutamate than GluK2, in that the channel opens, closes, and desensitizes faster than GluK2 does. The apparent difference in the channel-gating properties between GluK1 and GluK2 may be surprising, because the two subunits share ~80% sequence identity, and such extensive sequence homology generally suggests common properties.

The rapid kinetic characterization of the GluK1 kainate receptor that we have described here represents our continuing effort to characterize the similarities and differences in the channel-opening kinetic properties between the kainate and AMPA receptor subtypes. In a more significant way, the results from this study demonstrate that GluK1 receptors exhibit a much slower rate of channel opening in response to glutamate binding and a slower rate of closing the open channels than do AMPA receptors.<sup>17, 19, 30, 40, 41</sup> The desensitization rate constant of GluK1 is, however, comparable to those of AMPA receptors.<sup>17, 19, 30, 40, 41</sup> Specifically, the maximum  $k_{des}$  is much faster than that of either the flip or the flop isoform of the GluA1 AMPA receptor channel but is comparable to that of the GluA2Q<sub>flop</sub> AMPA receptor channel, which is much faster than GluA2Q<sub>flip</sub>. The  $K_I$  or  $EC_{50}$  values for both GluK1 and GluK2<sup>18, 21</sup> are comparable to that of the GluA1 AMPA receptor, but are about two-fold smaller than the corresponding values for the rest of the AMPA receptor homomeric channels<sup>17, 19, 30, 40, 41</sup>. Therefore, the results from this study and the studies we reported before<sup>18, 21</sup> support that kainate receptors (i.e., GluK1 and GluK2) have different channel properties as compared with AMPA receptors.

The results for GluK1, together with the results for GluK2,<sup>21</sup> show that kainate receptors are kinetically slower than AMPA receptors to open the channel. This conclusion may be useful in understanding the role of kainate receptors, which is much less understood than the role of AMPA receptors, in mediating synaptic plasticity.<sup>3, 5, 42</sup> For example, our results may account for the slower time course of the rise and decay of the kainate-mediated excitatory postsynaptic currents (EPSCs) than the AMPA receptor-mediated EPSCs, as observed in hippocampal CA3 pyramidal cells.<sup>43–45</sup> The time course of this mixed AMPA and kainate EPSCs is similar to those reported for synapses on CA1 hippocampal interneurons<sup>46, 47</sup> and in layer-IV neurons of the primary somatosensory cortex.<sup>48</sup> The difference in the channel-opening kinetic properties, defined by those rate constants, between kainate and AMPA receptors could be an explanation of different EPSC profiles.<sup>18</sup> Therefore, our results support the hypothesis that kainate receptors encode different ranges of afferent fiber frequency as compared with AMPA receptors.<sup>49–51</sup> A relatively slow kainate-receptor mediated EPSCs can be also ascribed to kinetic behaviors of heteromeric kainate

receptors.<sup>52</sup> It is known, for instance, that GluK1/GluK5 has different gating properties as compared with GluK1 homoeric channels.<sup>33</sup> Association of auxiliary proteins with kainate receptors is also known to slow the decaying of EPSCs<sup>53, 54</sup>. Therefore, similar studies of channel-opening kinetic properties of both heteromeric kainate channels and protein-kainate receptor complexes will be helpful for a better understanding of the kainate-receptor mediated synaptic neurotransmission.

## Supplementary Material

Refer to Web version on PubMed Central for supplementary material.

## Acknowledgments

We thank Peter Seeburg for the wild-type GluK1-2a DNA plasmid, and Geoffrey Swanson for the GluK1-2b DNA plasmids.

**Funding** This work was supported by grants from NIH/NINDS (R01 NS060812), Department of Defense (W81XWH-04-1-0106) and the Muscular Dystrophy Association (to L.N.).

## ABBREVIATIONS

<b>AMPA</b>	$\alpha$ -amino-3-hydroxy-5-methyl-4-isoxazolepropionic acid
<b>EPSCs</b>	excitatory postsynaptic currents
<b>ER</b>	endoplasmic reticulum
<b>HEK-293 cells</b>	human embryonic kidney 293 cells

## REFERENCES

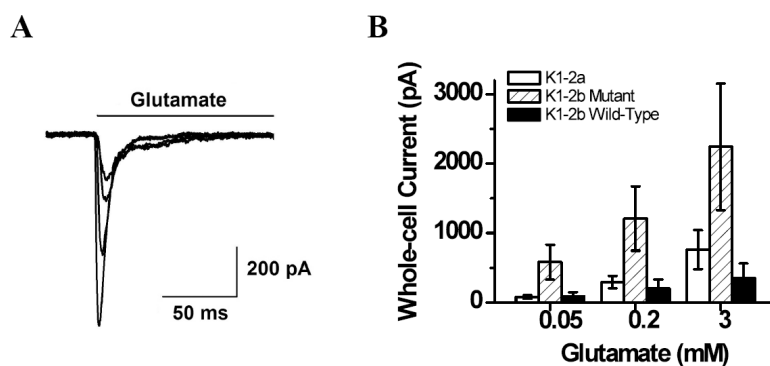
1. Contractor A, Mulle C, Swanson GT. Kainate receptors coming of age: milestones of two decades of research. *Trends Neurosci.* 2011; 34:154–163. [PubMed: 21256604]
2. Perrais D, Veran J, Mulle C. Gating and permeation of kainate receptors: differences unveiled. *Trends in pharmacological sciences.* 2010; 31:516–522. [PubMed: 20850188]
3. Jane DE, Lodge D, Collingridge GL. Kainate receptors: pharmacology, function and therapeutic potential. *Neuropharmacology.* 2009; 56:90–113. [PubMed: 18793656]
4. Dingledine R, Borges K, Bowie D, Traynelis SF. The glutamate receptor ion channels. *Pharmacol Rev.* 1999; 51:7–61. [PubMed: 10049997]
5. Lerma J. Kainate receptor physiology. *Curr Opin Pharmacol.* 2006; 6:89–97. [PubMed: 16361114]
6. Lerma J, Paternain AV, Rodriguez-Moreno A, Lopez-Garcia JC. Molecular physiology of kainate receptors. *Physiol Rev.* 2001; 81:971–998. [PubMed: 11427689]
7. Collingridge GL, Olsen R, Peters JA, Spedding M. Ligand gated ion channels. *Neuropharmacology.* 2009; 56:1. [PubMed: 18817790]
8. Bettler B, Boulter J, Hermans-Borgmeyer I, O'Shea-Greenfield A, Deneris ES, Moll C, Borgmeyer U, Hollmann M, Heinemann S. Cloning of a novel glutamate receptor subunit, GluR5: expression in the nervous system during development. *Neuron.* 1990; 5:583–595. [PubMed: 1977421]
9. Sommer B, Burnashev N, Verdoorn TA, Keinänen K, Sakmann B, Seeburg PH. A glutamate receptor channel with high affinity for domoate and kainate. *EMBO J.* 1992; 11:1651–1656. [PubMed: 1373382]
10. Ren Z, Riley NJ, Needleman LA, Sanders JM, Swanson GT, Marshall J. Cell surface expression of GluR5 kainate receptors is regulated by an endoplasmic reticulum retention signal. *J Biol Chem.* 2003; 278:52700–52709. [PubMed: 14527949]
11. Christensen JK, Varming T, Ahring PK, Jorgensen TD, Nielsen EO. In vitro characterization of 5-carboxyl-2,4-di-benzamidobenzoic acid (NS3763), a noncompetitive antagonist of GLUK5 receptors. *J Pharmacol Exp Ther.* 2004; 309:1003–1010. [PubMed: 14985418]

12. Swanson GT, Gereau R. W. t. Green T, Heinemann SF. Identification of amino acid residues that control functional behavior in GluR5 and GluR6 kainate receptors. *Neuron*. 1997; 19:913–926. [PubMed: 9354337]
13. Ritz M, Micale N, Grasso S, Niu L. Mechanism of inhibition of the GluR2 AMPA receptor channel opening by 2,3-benzodiazepine derivatives. *Biochemistry*. 2008; 47:1061–1069. [PubMed: 18161947]
14. Swanson GT, Green T, Heinemann SF. Kainate receptors exhibit differential sensitivities to (S)-5-iodowillardiine. *Mol Pharmacol*. 1998; 53:942–949. [PubMed: 9584222]
15. Swanson GT, Heinemann SF. Heterogeneity of homomeric GluR5 kainate receptor desensitization expressed in HEK293 cells. *J Physiol*. 1998; 513(Pt 3):639–646. [PubMed: 9824706]
16. Wieboldt R, Gee KR, Niu L, Ramesh D, Carpenter BK, Hess GP. Photolabile precursors of glutamate: synthesis, photochemical properties, and activation of glutamate receptors on a microsecond time scale. *Proc Natl Acad Sci U S A*. 1994; 91:8752–8756. [PubMed: 8090718]
17. Li G, Pei W, Niu L. Channel-opening kinetics of GluR2Q(flip) AMPA receptor: a laser-pulse photolysis study. *Biochemistry*. 2003; 42:12358–12366. [PubMed: 14567697]
18. Li G, Oswald RE, Niu L. Channel-opening kinetics of GluR6 kainate receptor. *Biochemistry*. 2003; 42:12367–12375. [PubMed: 14567698]
19. Li G, Niu L. How fast does the GluR1Qflip channel open? *J Biol Chem*. 2004; 279:3990–3997. [PubMed: 14610080]
20. Canepari M, Nelson L, Papageorgiou G, Corrie JE, Ogden D. Photochemical and pharmacological evaluation of 7-nitroindolyl- and 4-methoxy-7-nitroindolyl-amino acids as novel, fast caged neurotransmitters. *J Neurosci Methods*. 2001; 112:29–42. [PubMed: 11640955]
21. Han Y, Wang C, Park JS, Niu L. Channel-opening kinetic mechanism for human wild-type GluK2 and the M867I mutant kainate receptor. *Biochemistry*. 2010; 49:9207–9216. [PubMed: 20863077]
22. Mano I, Teichberg VI. A tetrameric subunit stoichiometry for a glutamate receptor-channel complex. *Neuroreport*. 1998; 9:327–331. [PubMed: 9507977]
23. Rosenmund C, Stern-Bach Y, Stevens CF. The tetrameric structure of a glutamate receptor channel. *Science*. 1998; 280:1596–1599. [PubMed: 9616121]
24. Jin R, Gouaux E. Probing the function, conformational plasticity, and dimer-dimer contacts of the GluR2 ligand-binding core: studies of 5-substituted willardiines and GluR2 S1S2 in the crystal. *Biochemistry*. 2003; 42:5201–5213. [PubMed: 12731861]
25. Mansour M, Nagarajan N, Nehring RB, Clements JD, Rosenmund C. Heteromeric AMPA receptors assemble with a preferred subunit stoichiometry and spatial arrangement. *Neuron*. 2001; 32:841–853. [PubMed: 11738030]
26. Sobolevsky AI, Rosconi MP, Gouaux E. X-ray structure, symmetry and mechanism of an AMPA-subtype glutamate receptor. *Nature*. 2009; 462:745–756. [PubMed: 19946266]
27. Loftfield RB, Eigner EA. Molecular order of participation of inhibitors (or activators) in biological systems. *Science*. 1969; 164:305–308. [PubMed: 4304859]
28. Lash LL, Sanders JM, Akiyama N, Shoji M, Postila P, Pentikainen OT, Sasaki M, Sakai R, Swanson GT. Novel analogs and stereoisomers of the marine toxin neodysiherbaine with specificity for kainate receptors. *J Pharmacol Exp Ther*. 2008; 324:484–496. [PubMed: 18032572]
29. Pei W, Ritz M, McCarthy M, Huang Z, Niu L. Receptor occupancy and channel-opening kinetics: a study of GLUR1 L497Y AMPA receptor. *J Biol Chem*. 2007; 282:22731–22736. [PubMed: 17545169]
30. Pei W, Huang Z, Wang C, Han Y, Park JS, Niu L. Flip and flop: a molecular determinant for AMPA receptor channel opening. *Biochemistry*. 2009; 48:3767–3777. [PubMed: 19275243]
31. Swanson GT, Green T, Sakai R, Contractor A, Che W, Kamiya H, Heinemann SF. Differential activation of individual subunits in heteromeric kainate receptors. *Neuron*. 2002; 34:589–598. [PubMed: 12062042]
32. Derkach V, Barria A, Soderling TR. Ca<sup>2+</sup>/calmodulin-kinase II enhances channel conductance of alpha-amino-3-hydroxy-5-methyl-4-isoxazolepropionate type glutamate receptors. *Proc Natl Acad Sci U S A*. 1999; 96:3269–3274. [PubMed: 10077673]

33. Swanson GT, Feldmeyer D, Kaneda M, Cull-Candy SG. Effect of RNA editing and subunit co-assembly single-channel properties of recombinant kainate receptors. *J Physiol.* 1996; 492(Pt 1): 129–142. [PubMed: 8730589]
34. Heckmann M, Bufler J, Franke C, Dudel J. Kinetics of homomeric GluR6 glutamate receptor channels. *Biophys J.* 1996; 71:1743–1750. [PubMed: 8889151]
35. Mayer ML. Crystal structures of the GluR5 and GluR6 ligand binding cores: molecular mechanisms underlying kainate receptor selectivity. *Neuron.* 2005; 45:539–552. [PubMed: 15721240]
36. Mayer ML, Ghosal A, Dolman NP, Jane DE. Crystal structures of the kainate receptor GluR5 ligand binding core dimer with novel GluR5-selective antagonists. *J Neurosci.* 2006; 26:2852–2861. [PubMed: 16540562]
37. Yan S, Sanders JM, Xu J, Zhu Y, Contractor A, Swanson GT. A C-terminal determinant of GluR6 kainate receptor trafficking. *J Neurosci.* 2004; 24:679–691. [PubMed: 14736854]
38. Clements JD, Lester RA, Tong G, Jahr CE, Westbrook GL. The time course of glutamate in the synaptic cleft. *Science.* 1992; 258:1498–1501. [PubMed: 1359647]
39. Colquhoun D, Jonas P, Sakmann B. Action of brief pulses of glutamate on AMPA/kainate receptors in patches from different neurones of rat hippocampal slices. *J Physiol.* 1992; 458:261–287. [PubMed: 1338788]
40. Li G, Sheng Z, Huang Z, Niu L. Kinetic mechanism of channel opening of the GluRDflip AMPA receptor. *Biochemistry.* 2005; 44:5835–5841. [PubMed: 15823042]
41. Pei W, Huang Z, Niu L. GluR3 flip and flop: differences in channel opening kinetics. *Biochemistry.* 2007; 46:2027–2036. [PubMed: 17256974]
42. Mellor JR. Synaptic plasticity of kainate receptors. *Biochem Soc Trans.* 2006; 34:949–951. [PubMed: 17052234]
43. Cossart R, Epsztein J, Tyzio R, Becq H, Hirsch J, Ben-Ari Y, Crepel V. Quantal release of glutamate generates pure kainate and mixed AMPA/kainate EPSCs in hippocampal neurons. *Neuron.* 2002; 35:147–159. [PubMed: 12123615]
44. Castillo PE, Malenka RC, Nicoll RA. Kainate receptors mediate a slow postsynaptic current in hippocampal CA3 neurons. *Nature.* 1997; 388:182–186. [PubMed: 9217159]
45. Vignes M, Bleakman D, Lodge D, Collingridge GL. The synaptic activation of the GluR5 subtype of kainate receptor in area CA3 of the rat hippocampus. *Neuropharmacology.* 1997; 36:1477–1481. [PubMed: 9517417]
46. Cossart R, Esclapez M, Hirsch JC, Bernard C, Ben-Ari Y. GluR5 kainate receptor activation in interneurons increases tonic inhibition of pyramidal cells. *Nat Neurosci.* 1998; 1:470–478. [PubMed: 10196544]
47. Frerking M, Malenka RC, Nicoll RA. Synaptic activation of kainate receptors on hippocampal interneurons. *Nat Neurosci.* 1998; 1:479–486. [PubMed: 10196545]
48. Kidd FL, Isaac JT. Developmental and activity-dependent regulation of kainate receptors at thalamocortical synapses. *Nature.* 1999; 400:569–573. [PubMed: 10448859]
49. Frerking M, Ohliger-Frerking P. AMPA receptors and kainate receptors encode different features of afferent activity. *J Neurosci.* 2002; 22:7434–7443. [PubMed: 12196565]
50. Sachidhanandam S, Blanchet C, Jeantet Y, Cho YH, Mulle C. Kainate receptors act as conditional amplifiers of spike transmission at hippocampal mossy fiber synapses. *J Neurosci.* 2009; 29:5000–5008. [PubMed: 19369569]
51. Goldin M, Epsztein J, Jorquera I, Represa A, Ben-Ari Y, Crepel V, Cossart R. Synaptic kainate receptors tune oriens-lacunosum moleculare interneurons to operate at theta frequency. *J Neurosci.* 2007; 27:9560–9572. [PubMed: 17804617]
52. Barberis A, Sachidhanandam S, Mulle C. GluR6/KA2 kainate receptors mediate slow-deactivating currents. *J Neurosci.* 2008; 28:6402–6406. [PubMed: 18562611]
53. Tang M, Pelkey KA, Ng D, Ivakine E, McBain CJ, Salter MW, McInnes RR. Neto1 is an auxiliary subunit of native synaptic kainate receptors. *J Neurosci.* 2011; 31:10009–10018. [PubMed: 21734292]

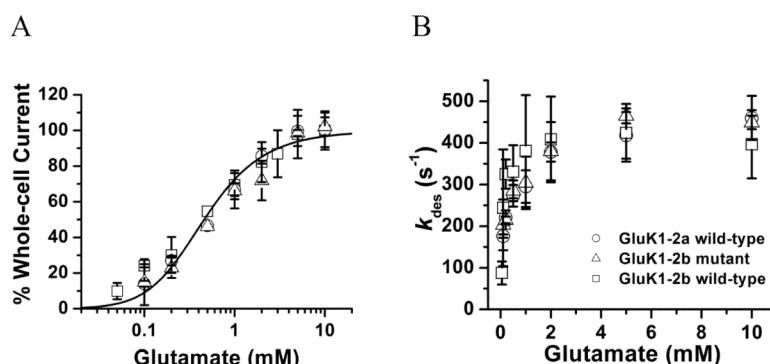
54. Straub C, Hunt DL, Yamasaki M, Kim KS, Watanabe M, Castillo PE, Tomita S. Distinct functions of kainate receptors in the brain are determined by the auxiliary subunit Neto1. *Nat Neurosci.* 2011; 14:866–873. [PubMed: 21623363]





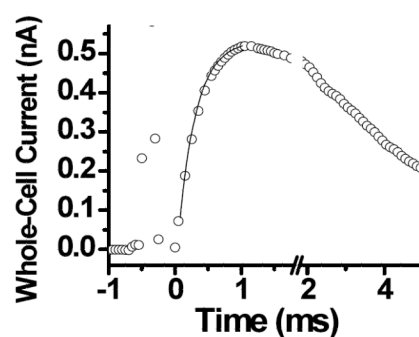
**FIGURE 1.**

(A) Representative traces of whole-cell current measured from a single HEK-293 cell expressing the mutant GluK1. Glutamate was applied at time zero, and the concentrations of glutamate were, from bottom up, 10, 1, 0.2 and 0.1 mM, respectively. (B) Average of the whole-cell current amplitudes of the wild-type GluK1-2a (hollow column), wild-type GluK1-2b (solid column) and the mutant GluK1-2b (shaded column). The number of cells used for comparison for each receptor was described in the text.

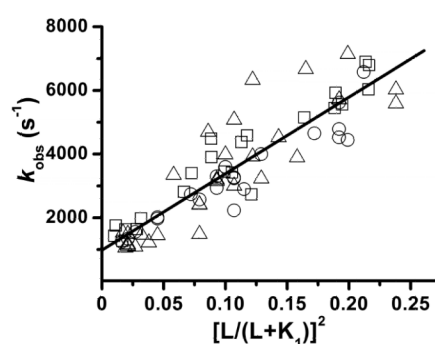
**FIGURE 2.**

(A) Dose-response relationship of the wild-type GluK1-2a (circle), wild-type GluK1-2b (square) and the mutant GluK1 receptors (triangle). Each data point is an average of at least three measurements from three different cells. A total of 53 cells were measured for the two wild-type and the mutant GluK1 receptors. The whole-cell current amplitudes from different cells were normalized to that of the control or 0.5 mM glutamate, and the average of the current amplitude collected from  $\geq 5$  mM glutamate concentrations was set to be 100%. The solid line is the nonlinear fit of the combined data based on eq 3 (see the detailed results of the fitting in Table 1). From the combined data, when  $n = 2$ ,  $K_I$  of  $480 \pm 50 \mu\text{M}$ ,  $\Phi$  of  $0.45 \pm 0.15$  and  $I_{MRM}$  of  $146 \pm 20$  were obtained. (B) Dependence of desensitization rate constant on glutamate concentration for the wild-type GluK1-2a (circle), wild-type GluK1-2b (square) and the mutant GluK1 receptors (triangle). Each data is an average of at least three data points from three cells.

A



B

**FIGURE 3.**

(A) A representative whole-cell current trace generated by the laser-pulse photolysis measurement with an HEK-293 cell expressing the wild-type GluK1-2a. A pulse of laser was fired at time zero. The concentration of glutamate released was estimated to be 180  $\mu\text{M}$ . A  $k_{obs}$  was calculated from the rising phase of the current to be  $3,300 \pm 76 \text{ s}^{-1}$  by using eq 1 (the solid line). Note that the current is plotted opposite to the direction that was recorded.

(B) Linear plot of the  $k_{obs}$  data combined from the two wild-type and mutant GluK1 receptors as a function of glutamate concentration by eq 2. Each data point represents a single  $k_{obs}$  value obtained at a particular concentration of photolytically released glutamate. Overall, a total of 20, 22 and 30 cells were measured for the wild-type GluK1-2a (circle), wild-type GluK1-2b (square) and the mutant GluK1-2b (triangle), respectively. The best linear fit yielded, at  $n = 2$ ,  $k_{op}$  and  $k_{cl}$  of  $(2.4 \pm 0.1) \times 10^4 \text{ s}^{-1}$  and  $(1.0 \pm 0.2) \times 10^3 \text{ s}^{-1}$ , respectively.

**Table 1**

Nonlinear fitting of the dose-response curve for the wild-type and mutant GluK1

$n^a$	$K_I$ (nM)	$\Phi$	$I_M R_M$ (nA)	$R^2$
1	$1.63 \pm 0.16$	$0.51 \pm 0.05$	$161 \pm 7$	0.99
2	$0.48 \pm 0.05$	$0.45 \pm 0.15$	$146 \pm 20$	0.97
3	$0.26 \pm 0.06$	$0.38 \pm 0.16$	$137 \pm 22$	0.95
4	$0.18 \pm 0.03$	$0.43 \pm 0.21$	$142 \pm 28$	0.94

<sup>a</sup>  $n$  was fixed as an integer.

**Table 2**Fitted  $k_{op}$  and  $k_{cl}$  with different  $n$  values for the wild-type and mutant GluK1

$n^a$	$k_{op} (\times 10^4 \text{ s}^{-1})$	$k_{cl} (\times 10^3 \text{ s}^{-1})$	$R^2$
1	$1.5 \pm 0.1$	$-0.7 \pm 0.2$	0.91
2	$2.6 \pm 0.1$	$1.1 \pm 0.2$	0.91
3	$5.5 \pm 0.3$	$1.7 \pm 0.1$	0.89
4	$11.7 \pm 0.8$	$2.1 \pm 0.1$	0.85

<sup>a</sup>  $n$  was chosen as an integer, and  $K_I$  was chosen to be 480  $\mu\text{M}$

**Table 3**Nonlinear fitting of the wild-type and mutant GluK1 data for estimating  $n$ ,  $k_{op}$  and  $K_I$ 

$k_{cl}^a$ (s <sup>-1</sup> )	<b>n</b>	$k_{op}$ ( $\times 10^3$ s <sup>-1</sup> )	$K_I$ (mM)	$R^2$
400	$1.8 \pm 0.4$	$2.7 \pm 0.4$	$0.44 \pm 0.17$	0.80
600	$1.9 \pm 0.5$	$2.6 \pm 0.3$	$0.44 \pm 0.16$	0.81
800	$2.0 \pm 0.6$	$2.4 \pm 0.3$	$0.43 \pm 0.15$	0.83
1000	$2.1 \pm 0.5$	$2.3 \pm 0.3$	$0.43 \pm 0.15$	0.83
1200	$2.0 \pm 0.5$	$2.5 \pm 0.4$	$0.48 \pm 0.15$	0.84
1400	$2.0 \pm 0.6$	$2.5 \pm 0.4$	$0.51 \pm 0.17$	0.82

<sup>a</sup>  $k_{cl}$  is fixed as specified